Biomedicine & Pharmacotherapy 137 (2021) 111372

Contents lists available at ScienceDirect

Biomedicine & Pharmacotherapy

journal homepage: www.elsevier.com/locate/biopha

Original article

The lignan-rich fraction from *Sambucus Williamsii* Hance ameliorates dyslipidemia and insulin resistance and modulates gut microbiota composition in ovariectomized rats

Hui-Hui Xiao [a,b,*,1], Lu Lu [a,1], Christina Chui-Wa Poon [b], Chi-On Chan [b], Li-Jing Wang [a], Yu-Xin Zhu [a], Li-Ping Zhou [b], Sisi Cao [b], Wen-Xuan Yu [b], Ka Ying Wong [b], Daniel Kam-Wah Mok [a,b], Man-Sau Wong [a,b,*]

[a] State Key Laboratory of Chinese Medicine and Molecular Pharmacology (Incubation), The Hong Kong Polytechnic University Shenzhen Research Institute, Shenzhen 518057, PR China

[b] Department of Applied Biology and Chemical Technology, The Hong Kong Polytechnic University, Hong Kong, China

ARTICLE INFO

Keywords:
Lignan-rich fraction
Sambucus williamsii Hance
Dyslipidemia
Insulin resistance
Ovariectomized rat
Actinobacteria

ABSTRACT

Menopausal women are susceptible to have high risk of cardiovascular diseases, type II diabetes and osteoporosis due to the metabolic disorder caused by estrogen deficiency. Accumulating evidence supports that gut microbiota is a key regulator of metabolic diseases. Our previous metabolomics study interestingly demonstrated that the anti-osteoporotic effects of lignan-rich fraction (SWCA) from *Sambucus wialliamsii* Hance were related to the restoration of a series of lipid and glucose metabolites. This study aims to investigate how SWCA modulates lipid and glucose metabolism and the underlying mechanism. Our results show that oral administration of SWCA (140 mg/kg and 280 mg/kg) for 10 weeks alleviated dyslipidemia, improved liver functions, prevented glucose tolerance and insulin actions, attenuated system inflammation and improved intestinal barrier in OVX rats. It also induced a high abundance of *Actinobacteria*, and restored microbial composition. We are the first to report the protective effects of the lignan-rich fraction from *S. williamsii* on dyslipidemia and insulin resistance. Our findings provide strong evidence for the application of this lignan-rich fraction to treat menopausal lipid disorder and insulin resistance-related diseases.

1. Introduction

Menopause is a natural event characterized by ovarian atrophy and dramatic decline in estrogen levels; it is a new phase of women's lives that starts around the age of 45–55. Many physiological and pathological modifications occur during this transition. Menopausal women are susceptible to body weight gain, lipid metabolism alternation, insulin resistance, hypertension, and bone loss due to the metabolic disorder caused by estrogen deficiency, which results in a high risk of cardiovascular diseases, type II diabetes and osteoporosis [1,2].

It's well known that cholesterol is a precursor of the formation of steroid hormones, therefore, the deficiency of oestrogen during menopause leads to an increase of serum cholesterol, and subsequently induces a high level of low density lipoprotein cholesterol (LDL-c), total cholesterol (TC) and triglyceride (TG), and a low level of the high density lipoprotein cholesterol (HDL_c) [3,4]. The accumulations of these lipids in serum, the liver and the pancreas adversely affect the functions of the liver and pancreas that further aggravates dyslipidemia and insulin resistance. It is of great importance to prevent the occurrence of metabolic disorder during the menopausal period to lower the risk of cardiovascular diseases and diabetes.

Physical exercise (45.4%), pharmacological treatment (36.4%) and diet (18.2%) are the most commonly used methods to treat menopausal women who are with dyslipidemia and susceptible to insulin resistance [5]. Bezafibrate [6], dehydroepiandrosterone [7], raloxifene [8] and statins [9] have been used to decrease insulin resistance or lipid levels in postmenopausal women. However, these drugs only play a limited therapeutic role in the complex metabolic disorders. They also cause some harmful side effects [3,10,11] and their therapeutic effects are lowered over long-term use [5]. There is an urgent need to search for

* Corresponding authors at: Department of Applied Biology and Chemical Technology, The Hong Kong Polytechnic University, Hong Kong, China.
E-mail addresses: huihui.xiao@polyu.edu.hk (H.-H. Xiao), bcmswong@polyu.edu.hk (M.-S. Wong).

[1] These authors have contributed equally to this work and share first authorship.

https://doi.org/10.1016/j.biopha.2021.111372
Received 10 November 2020; Received in revised form 25 January 2021; Accepted 31 January 2021
Available online 22 February 2021

more desirable alternative and complementary medicines for controlling the metabolic disorders during menopause.

In the theory of Traditional Chinese Medicine (TCM), menopausal metabolic symptoms are attributed to "Kidney deficiency" [12]. There is accumulating evidence indicating that the extracts of certain single herbs or herbal formula could lower dyslipidemia [13,14] and attenuate insulin resistance [15,16]. *Sambucus williamsii* Hance, a folk Chinese medicine, has been traditionally used to treat bone fractures, rheumatoid arthritis, inflammation-related gastrointestinal disorders and kidney diseases for thousands of years [17]. It exhibits various pharmacological activities, such as anti-inflammatory [18], anti-osteoporosis [19], antioxidant [20], and hepatoprotective effects [21]. In addition, the linoleic acid isolated from *S. williamsii* seed oil was reported to exhibit anti-glycemic and anti-hypolipidemic properties [20]. However, the effects of ramulus, the traditional medicinal part of *S. williamsii*, on diseases related to lipid and glucose metabolism are still unknown. Our previous metabolomics study interestingly demonstrated that the bone protective effects of the lignan-rich fraction (SWCA) from *S. wialliamsii* were related to the restoration of a series of lipid and glucose metabolites, such as lysoPC (22:5), lysoPC (22:6), lysoPC (22:4), lysoPC (18:0), arachidonic acid (C20:4), linoleic acid (C18:2), and oleic acid (C18:1) in aged ovariectomized rats [22]. However, how SWCA modulates lipid and glucose metabolism and the underlying mechanism are still unclear.

There are more than 10^{14} microorganisms host, including bacteria, archaea and fungi, on the surface of the human gastrointestinal tract [23]. Since the implementation of Human Microbiome Project funded by National Institutes of Health, there has been accumulating evidence supporting that gut microbiota is a key regulator of metabolic diseases, such as obesity, type 2 diabetes and cardiovascular diseases [24–28]. It has been reported that metabolic status changes in host could induce the alternation of gut microbial composition, leading to increase in some pathogenic bacteria, which subsequently disrupts the gut barrier, increases gut permeability and promotes the production of endotoxin, eventually resulting in inflammation and consequently causing insulin resistance, hyperlipidemia and obesity [29]. Thus, gut microbiota has been suggested to be a potential drug target for both prevention and treatment of metabolic diseases.

In this study, rats with ovariectomy-induced metabolic disorders were employed to investigate the preventive effects of SWCA on dyslipidemia and insulin resistance. The inflammatory, gut barrier and gut microbiota altered by SWCA were also determined to explore the underlying mechanism of its actions.

2. Materials and methods

2.1. Plant material, preparation and LC-MS quantitation of lignan-rich fraction from S. williamsii

The stem branches of *S. williamsii* were collected in Xinbin City, Liaoning Province in the northeast of China in May 2017 and authenticated according to a method listed in Chinese Bencao with the help of Professor Sibao Chen (Shenzhen Research Institute of the Hong Kong Polytechnic University, Shenzhen, China). A voucher specimen (SWSZ-2017) was deposited in the Shenzhen Institute of the Hong Kong Polytechnic University (Shenzhen, China).

The dried stems and branches of *S. williamsii* (150 kg) were refluxed with 1200 liters of 60% (v/v) ethanol twice, each time for 2 h. After filtration, the filtrate was concentrated to 150 L under reduced pressure, subjected to a HP-20 macroporous absorptive resin column, and eluted with water and ethanol in gradient to give a lignan-rich fraction SWCA (50% ethanol-aqua eluate, 396 g) [30].

The content of the major components in SWCA was determined by LC-MS method. Four lignans that were isolated, purified and identified as reported in our previous studies, namely (7R,8S)−2,3-dihydro-2-(4–hydroxy-3-methoxyphenyl)−7-methoxy-5-(3-methoxy-1-(propenyl)−3-benzofuranomethanol (M1), Tetrahydrodehydrodiconiferyl alcohol (M2), 7-hydroxy-secoisolariciresinol (M3), Secoisolariciresinol (M4) [30], were selected as markers in this study.

The analysis of SWCA solution and the four markers was performed using an ACQUITY UPLC H-Class system coupled to a Xevo TQD mass spectrometer (Waters Corp., Milford, USA). A Waters UPLC BEH C18 column (1.7 μm, 2.1 × 50 mm; Waters Corp. Milford, USA) was applied for LC separation. The mobile phases consisted of A (10 mM Ammonium formate water) and B (acetonitrile) at a flow rate of 0. 3 ml/min with elution gradients as follows: 0–8 min, 10%−20%B; 8–10 min, 20%−25%B; 10–15 min, 25%−95%B; 15–15.5 min 95%−10%B; 15.5−20 min, 10%B. Column and sample chamber temperature were set at 40 °C and 5 °C, respectively. Mass spectrometry was operated in an electrospray ion source in positive multiple reaction monitoring (MRM) mode. The analytical parameters were set as follows: desolvation temperature, 350 °C; source gas flow, 650 L/H; cone gas flow, 40 L/H. The details of collision energy of each compound and their parent ions and daughter ions were listed in Table 1. The contents of the four markers in SWCA were 41.2, 27.2, 8.6 and 6.3 mg/g, respectively.

2.2. Animals and their treatment

Sprague-Dawley (SD) female rats (4 months old) were purchased from Beijing Vital River Laboratory Animal Technology Co., Ltd. and housed in the standard condition of 23 ± 2 °C temperature, 40–60% humidity and an alternating light and dark cycle (12 h light/12 h dark). The animal welfare and all experimental protocols (No.180402) were strictly in accordance with the procedures approved by the Animal Ethic Committee of The Hong Kong Polytechnic University. During the study, all rats were allowed free access to distilled water and pair-fed the phytoestrogen-free diet (D00031602, Research Diet, NJ, USA). The phytoestrogen-free diet was applied in the present study to eliminate interactions between diet and SWCA as described in our previous study [31].

After inspection and quarantine for 5 days, the rats were sham-operated or ovariectomized. After recovery for 10 days, the rats were randomly divided into five groups: sham + vehicle group (Sham, n = 10), OVX + vehicle group (OVX, n = 10), OVX + parathyroid hormone group (1.8 μg/kg, PTH, n = 8), OVX + SWCA low-dose group (140 mg/kg, CAL, n = 10) and OVX + SWCA high-dose group (280 mg/kg, CAH, n = 10). Ultrapure water was used as the vehicle. For the known lipolytic actions of PTH in adipose tissue of human [32,33], PTH was chosen as the positive control in this study. After oral administration of these drugs for 10 weeks, the rats were anesthetized by intraperitoneal injection of chloral hydrate (5%, 0.7 ml/100 g). The blood was withdrawn from the abdominal aorta of the rats, centrifuged at 3000 rpm, 4 °C for 10 min to get serum, then the serum was stored at −80 °C. The uterus was collected and weighed, a part of the liver was stored at −80 °C, and another part of the liver and colon were collected and fixed in 10% formalin for further histomorphometric and immunohistological analysis.

2.3. Analyses of biochemical indexes and proinflammatory cytokine

The concentrations of serum triglyceride (TG), total cholesterol (TC), alanine aminotransferase (ALT), aspartate aminotransferase (AST), total bilirubin (TBil), albumin (ALB) and fasting serum glucose (FSG) were

Table 1
Mass spectra properties of four markers in SWCA.

	Parent (m/z)	Daughter (m/z)	Cone (V)	Collision (V)
M1	331.2	287.1	25	10
M2	345.2	221.1	25	8
M3	325.2	163.1	20	17
M4	327.2	163.0	30	15

determined according to the procedure described in the commercial kits (KHB, Shanghai, China) using a 7100 automatic biochemistry analyzer (Hitachi Ltd., Tokyo, Japan). The 10% liver homogenate was prepared in saline using homogenizer at 4 °C. The homogenate was centrifuged at 3000 rpm for 15 min and the supernatant was used for the liver lipid assay.

Serum levels of fasting insulin (FINS), interleukin-1β (IL-1β), interleukin-1α (IL-1α), monocyte chemoattractant protein-1(MCP-1), interleukin-6 (IL6), interleukin-22 (IL-22) and tumor necrosis factor α (TNF-α) were detected with commercial enzyme linked immunosorbent assay (ELISA) kits (R&B Co. Ltd., MN, USA) according to the manufacturer's protocol.

2.4. Insulin resistance and sensitivity assay

Insulin is essential for fat and protein metabolism and glucose homeostasis. Insulin resistance underlies the characteristic features of postmenopausal dyslipidemia [34]. Therefore, we used the oral glucose tolerant test (OGTT) and homeostasis model assessment (HOMA) to assess insulin resistance and insulin sensitivity.

OGTT, which assesses the disposal of orally administrated glucose load and insulin secretion over time, is useful to characterize metabolic phenotypes and investigate alternation in glucose metabolism. After treatment for 8 weeks, the rats were fasted overnight (14 h) but were allowed access to water before testing. Then the rats were carefully administrated with a glucose solution (2.5 g/kg) via gavage according to a previous study [35]. Blood was collected at the time points of 0, 30, 60, 90, and 120 min from the rat tail-tip, and blood glucose levels were measured with a Accu-Chek Guide Me meter (Roche Diabetes Care, Inc, IN, USA). The area under the glucose curve (AUC) was calculated based on the blood glucose curve.

Homeostasis model assessment (HOMA), which was first proposed by Turner's research team at the University of Oxford in 1985, is a widely used method in clinical evaluation of insulin resistance, insulin levels, and pancreatic islet beta cell functions. It includes HOMA-insulin resistance (HOMA-IR), homeostasis model assessment-β (HOMA-β) and HOMA-insulin sensitivity (HOMA-IS) [36]. The specific formula is as follows: HOMA-IR =(FSG x FINS)/22.5; HOMA β-cell =(20x FINS) / (FSG-3.5) x 100%; HOMA-IS= 22.5 / (FSG x FINS).

2.5. Rat liver and colon histomorphometric and immunohistological analysis

Fresh liver and colon were fixed in 10% formalin, processed and embedded in paraffin, and cut into 3 μm thick slices. Tissue sections were stained with hematoxylin and eosin (H&E) and examined using a light microscope equipped with a CCD camera (Nikon Co.,Ltd., Tokyo, Japan) at 100 ×, 200 × and 600 × magnification.

Immunohistological analysis was performed on the formalin-fixed, paraffin-embedded tissue sections using primary antibodies of anti-TNF-α, anti-IL-22 (1:500 dilutions; Abcam, Cambridge, MA, USA) for liver and colon, and anti-ZO1, anti-Claudin-2 and anti-Occludin (1:500 dilutions; Abcam, Cambridge, MA, USA) for colon. After incubation with horseradish peroxidase (HRP)-labeled secondary antibody (Santa Cruz, CA, USA), the sections were stained with DAB chromogen kit and then counterstained with hematoxylin. The stained sections were viewed with a Nikon Ni-U fluorescence microscopes (Germany) and analyzed using Image-Pro Plus software (Media Cybernetics, USA).

2.6. Feces sample collection and DNA extraction

Fresh fecal samples from rats were collected after treatment for 10 weeks. Total DNA was extracted from 0.2 g fecal sample using the Stool Genomic DNA Extraction Kit (Solarbio Life Sciences, Beijing, China) according to the manufacturer's instruction. The concentration of bacterial DNA was determined by Qubit Fluorometer (Thermo Scientific, USA) and DNA quality was checked by 1% agarose gel electrophoresis.

The V3-V4 hypervariable regions of the bacteria 16S rRNA gene were amplified with primers 338F (5′-ACTCCTACGGGAGGCAGCAG-3′) and 806R (5′-GGACTACHVGGGTWTCTAAT-3′) by the thermocycler PCR system (GeneAmp 9700, ABI, USA). The PCR reactions were conducted using the following program: 3 min of denaturation at 95 °C, 27 cycles of 30 s at 95 °C, 30 s for annealing at 55 °C, and 45 s for elongation at 72 °C, and a final extension at 72 °C for 10 min. The resulted PCR products were extracted from 2% agarose gel and further purified using the AxyPrep DNA Gel Extraction Kit (Axygen Biosciences, Union City, CA, USA) and quantified using QuantiFluor™-ST (Promega, USA) according to the manufacturer's protocol.

2.7. 16S rRNA gene Illumina sequencing and analyses

Purified amplicons were pooled in equimolar and paired-end sequenced on an Illumina MiSeq platform (Illumina, CA, USA) according to the standard protocols by Majorbio Bio-Pharm Technology Co. Ltd. (Shanghai, China). Pairs of reads from the original DNA fragments were merged using fast length adjustment of short reads (FLASH 1.2.11, https://ccb.jhu.edu/software/FLASH/index.shtml) software, and sequences were analyzed using quantitative insights into microbial ecology (QIIME 1.9.1) software. A total of 1,562,176 high-quality sequence reads were generated from the amplicon library. The sequences were clustered into 899 operational taxonomic units (OTU) at a similarity level of 97% using UPARSE (version 7.0 http://qiime.org/install/index.html).

All statistical analyzes were performed using R packages (V.2.15.3) [38,39]. Bacterial richness and diversity across samples were assessed using the following α indexes, which were estimated at a distance of 3%: Chao, Ace, Simpson, Shannon, Sobs and coverage. Partial Least Squares Discriminant analysis (PLS-DA) was performed to compare bacterial composition and sharpen the separation between groups of observations. LEfSe analysis was employed to identify distinguishing taxa among different groups at multiple levels and to visualize the results using taxonomic bar charts and cladograms. The Kruskal-Wallis H test was used to evaluate group differences. The Spearman's correlation coefficients were used to assess bivariate relationships between variables. Results with $P < 0.05$ between groups were considered statistically significant.

2.8. Statistical analysis

The pharmacodynamic data were presented as mean ± SEM. Differences were statistically analyzed with one-way analysis of variance (ANOVA) followed by Tukey's post-hoc test using by GraphPad PRISM software package 6. $P < 0.05$ was considered statistically significant.

3. Results

3.1. SWCA does not influence body weight gain

As shown in Fig. 1A and B, there were no significant differences in the initial body weight of any of the rats, while the body weight of the OVX group was significantly heavier than that of the Sham group starting from the fourth week of the experiment even the two groups were pair-fed of 15 g diet per day. Compared with OVX group, PTH and SWCA treatment showed no significant weight gain at 4, 8 and 10 weeks. The body weight change (%, body weight gain/body weight at 0 week) of the OVX group significantly increased compared with the Sham group, while drug treatments had no effects on the body weight of OVX rats (Fig. 1C).

3.2. SWCA alleviates the ovariectomy-induced dyslipidemia

The levels of TC, TG, HDL-C and LDL-C in both serum and liver were

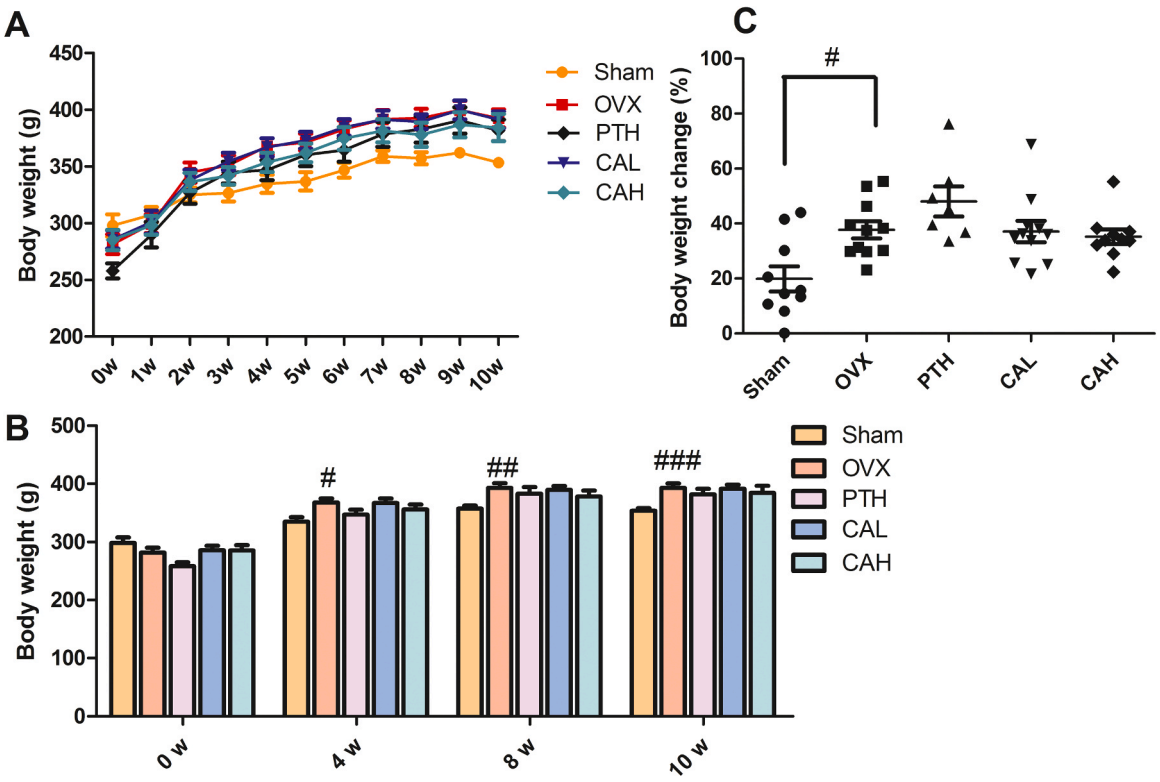

Fig. 1. Effects of SWCA on body weight gain in ovariectomized rats. (A) weekly body weight; (B) the body weight at weeks 0, 4, 8, and 10; (C) the net body weight gain. Four-month-old SD rats were subjected to the following treatment for 10 weeks after ovariectomy: Sham, Sham-operated, vehicle-treated, $n = 10$; OVX, ovariectomized, vehicle-treated, $n = 10$; PTH, ovariectomized, 1.8 μg/kg, $n = 8$; CAL, ovariectomized, low-dose SWCA fraction (140 mg/kg), $n = 10$; CAH, ovariectomized, high-dose SWCA fraction (280 mg/kg), $n = 10$. Results were expressed as mean ± SEM. # $P < 0.05$, ## $P < 0.01$, ### $P < 0.001$ versus Sham by One-Way ANOVA followed with the Tukey's post-hoc test.

determined and shown in Table 2. Ovariectomy resulted in significant increases in TC, TG, and LDL-C in serum and liver, indicating that lipid metabolism was significantly impaired after OVX surgery. The LDL-C in serum, TC and TG in liver were significantly decreased in OVX rats upon PTH treatment. Similarly, in response to SWCA treatment (at the dosage of 140 mg/kg for 10 weeks), the changes in TC and LDL-C in both serum and liver as well as TG in liver were significantly restored. The high dosage of SWCA showed improving trends in all these parameters but without statistical significance.

3.3. SWCA improves liver functions

As shown in Table 2, serum levels of ALT, AST, TBil, ALB in the OVX group were significantly higher than those of the Sham group, which

Table 2
Effects of SWCA on serum and liver lipids in ovariectomized rats.

Group	Sham	OVX	PTH	CAL	CAH
S-TC(mg/dL)	2.11 ± 0.10	2.64 ± 0.15##	2.35 ± 0.09	2.06 ± 0.08**	2.34 ± 0.07
S-TG(mmol/L)	0.50 ± 0.04	0.71 ± 0.06#	0.60 ± 0.03	0.54 ± 0.03*	0.62 ± 0.04
S-LDL-C(mmol/L)	0.58 ± 0.05	0.86 ± 0.07##	0.62 ± 0.05*	0.57 ± 0.03**	0.67 ± 0.04
S-HDL-C(mmol/L)	0.15 ± 0.04	0.08 ± 0.02	0.07 ± 0.02	0.14 ± 0.03	0.19 ± 0.03
L-TC(mg/dL)	0.54 ± 0.10	1.31 ± 0.13###	0.63 ± 0.11**	0.68 ± 0.12**	0.89 ± 0.14
L-TG(mmol/L)	1.88 ± 0.29	7.18 ± 1.20###	3.07 ± 0.59**	3.53 ± 0.69*	4.59 ± 0.92
L-LDL-C(mmol/L)	0.16 ± 0.02	0.36 ± 0.08#	0.19 ± 0.05	0.15 ± 0.01*	0.19 ± 0.03
L-HDL-C(mmol/L)	0.35 ± 0.04	0.19 ± 0.03	0.43 ± 0.05*	0.35 ± 0.09	0.23 ± 0.02
AST(U/L)	125.8 ± 11.7	180.2 ± 13.9##	113.0 ± 11.0***	130.4 ± 5.0**	112.7 ± 6.1***
ALT(U/L)	31.6 ± 1.6	47.7 ± 1.5###	29.9 ± 2.3***	37.3 ± 2.1**	34.3 ± 2.8***
AST/ALT	3.97 ± 0.28	3.81 ± 0.31	3.87 ± 0.40	3.55 ± 0.15	3.43 ± 0.18
TBIL(%)	1.29 ± 0.08	1.77 ± 0.10#	1.70 ± 0.14	1.79 ± 0.07	2.04 ± 0.17
ALB(g/L)	32.2 ± 0.4	36.3 ± 1.3##	31.0 ± 0.4***	30.4 ± 0.6***	30.3 ± 0.4***

Four-month-old SD rats were subjected to the following treatment for 10 weeks after ovariectomy: Sham, Sham-operated, vehicle-treated; OVX, ovariectomized, vehicle-treated; PTH, ovariectomized, 1.8 μg/kg; CAL, ovariectomized, low-dose SWCA fraction (140 mg/kg), $n = 10$; CAH, ovariectomized, high-dose SWCA fraction (280 mg/kg). "S-" indicated serum; "L-" indicated liver. Results were expressed as mean ± SEM.

# $P < 0.05$,
$P < 0.01$,
$P < 0.001$ versus Sham group,
* $P < 0.05$,
** $P < 0.01$,
*** $P < 0.001$ versus OVX group by One-Way ANOVA.

indicated the impairment of live function after ovariectomy. After treatment for 10 weeks, the levels of ALT, AST and ALB of SWCA were significantly improved compared with the OVX group, and the results of SWCA was similar to that of PTH treatment. The ratio of AST/ALT was consistent in all groups.

The H&E staining of liver was performed. As shown in Fig. 2, the livers of the Sham rats showed normal hepatic histology with normal hepatocytes, and without cell enlargement, inflammation, lipid droplets, or necrosis. The livers of the OVX rats showed steatosis with cytoplasmic lipid vacuoles and inflammatory cell infiltrates, while treatment of SWCA at both dosages reversed this steatosis.

3.4. SWCA prevents ovariectomy-induced impairments of glucose tolerance and insulin actions

Whole body glucose clearance during OGTT on the fasting rats was determined after treatment for 8 weeks. Fig. 3A presents the time course of absolute glucose levels during the OGTT. OVX rats had significant increased glucose concentrations at 30, 60, 90 and 120 min compared with the Sham group, indicating that ovariectomy induced glucose resistance. Treatment with PTH, and both low and high dosage of SWCA could significantly reverse these impairments induced by ovariectomy. The AUC above baseline glucose was calculated to validate the results (Fig. 3B). Compared with Sham rats, ovariectomy induced incremental glucose AUC by 12%, while treatment of SWCA at both dosages reversed this impairment of glucose clearance.

The circulating blood FSG and FINS were determined after two weeks of OGTT (Fig. 3C and D). The levels of FSG and FINS in OVX rats were significantly increased compared with those of the Sham group, while the levels in OVX rats were significantly decreased in response to the treatment of PTH, low or high dosage of SWCA. To measure insulin resistance, insulin sensitivity and pancreatic islet beta cell function, the HOMA was analyzed based on FSG and FINS. As shown in Fig. 3E–G, ovariectomy significantly stimulated insulin resistance and suppressed insulin sensitivity, while it did not influence the functions of pancreatic islet beta cell. SWCA treatment at both dosages, similar to the effects of PTH, significantly reversed the abnormal alternations of insulin induced by ovariectomy.

3.5. SWCA attenuates systemic inflammation induced by ovariectomy

The levels of TNF-α, IL-6, IL-1β, IL-1α, MCP1 and IL-22, which are proinflammatory cytokines with important functions in dyslipidemia, were determined in serum, liver and colon in the current study. As shown in Fig. 4A, the serum levels of TNF-α and IL-22 were significantly increased in the OVX group compared with the Sham group, and this increase was significantly reversed by PTH and SWCA treatments. Compared with Sham rats, the MCP-1 level showed increased trend in OVX rat, while treatment with CAL significantly decreased the MCP-1 level in OVX rats. There were no significant alternations of IL-1β, IL-1α and IL-6 in the Sham, OVX or SWCA treatment groups.

The immunohistological results of liver and colon (Fig. 4B) showed that the expressions of TNF-α were significantly increased in the OVX group compared with the Sham group, while treatment with SWCA, similar to PTH treatment, significantly decreased these expressions of TNF-α in OVX rats. Interestingly, the expressions of IL-22 were significantly decreased in both the liver and colon of OVX rats, while SWCA treatment reversed these changes.

3.6. SWCA prevents ovariectomy-induced impairment of the colon

As the integrity of the intestinal barrier is a key characteristic related to the inflammatory conditions of metabolic diseases, the epithelial tight junction proteins in the colon were determined in this study. As shown in Fig. 5A, there were no obvious differences in the histological features of the colon among all the groups. Immunohistological analysis (Fig. 5A and B) showed that ovariectomy significantly reduced the protein expressions of zonula occludens-1 (ZO-1), claudin-2 and occludin compared with the Sham group. CAL treatment significantly promoted the expressions of these tight junction proteins in OVX rats, while PTH treatment only brought about some increasing trends in these proteins.

3.7. Gut microbiota composition and structural changes in response to SWCA treatment

As our previous study indicated that gut microbiota might be involved in the actions of the lignan-rich fraction of *S. williamsii* in modulating the metabolic changes in the serum of ovariectomized rats [22], gut microbiota was sequenced on an Illumina MiSeq platform in the present study. The gut microbiota of all samples were classified as 901 OTUs, 318 species, 170 genera, 58 families, 36 orders, 22 classes and 12 phyla based on the sequencing data. Ovariectomized rats showed lower numbers of genus and species compared with the Sham rats, while treatment with low dosage of SWCA reversed these changes (Supplementary Table S1). The alpha diversity analysis of ace index, chao index, sobs index, shannon index, simpson index and coverage index showed that the CAL treatment group had significantly increased Sobs and Chao indexes compared with the Sham and OVX groups as shown in Supplementary Table S2. The results indicated that CAL treatment was able to increase microbial community richness.

The top nine phyla of the gut microbiota in each group were *Firmicutes*, *Bacteroidetes*, *Proteobacteria*, *Verrucomicrobia*, *Tenericutes*, *Elusimicrobia*, *Actinobacteria*, *Cyanobacteria* and *Lentisphaerae* (Fig. 6A). There were no significant differences in the relative abundances of these phyla between the Sham and OVX groups, while the CAL treatment group had significantly increased abundance of *Actinobacteria* compared with both the Sham and OVX groups. Although the ratio of *Firmicutes/Bacteroidetes* (F/B) increased in OVX rats compared with the Sham rats, and it was slightly decreased in OVX rats in response to CAL treatment, these differences had no statistical significance. *Actinobacteria was* significantly increased in the SWCA treatment group compared with both the Sham and OVX groups. To assess specific changes in the gut microbiota, the relative abundance of microbiota at the genus level were analyzed using Kruskal-Wallis H test. The top 15 genera with significant differences in analysis between Sham, OVX and CAL were shown in Fig. 6B. Compared with the Sham group, ovariectomy significantly promoted the increase of the relative abundance of *Ruminococcaceae_UCG-014* and *[Eubacterium]_coprostanoligenes_group* while CAL treatment significantly reversed these changes. In addition, CAL treatment significantly increased the abundances of *Lachnoclostridium*, *Anaerotruncus*, *Lachnospiraceae_UCG-010*, *Adlercreutzia*, *Enterococcus*, *Barnesiella* and *Lachnospiraceae_Nk4b4_group* in OVX rats, although these genera only showed decreasing trends in OVX rats compared with the Sham group.

In order to identify special communities of microbiota, the clade of microbial community from phylum to genus level was analyzed by LEfSe tool. Groups were shown as cladograms in Fig. 7A and LDA scores (>2) in Fig. 7B. Upon CAL treatment, two series of microbes were significantly enriched (Fig. 7A), namely, 1) phylum: *Actinobacteria* → class: *Actinobacteria* → order: *Coriobateriates* → family: *Coriobacteriaceae* → genus: *Adlercreutzia, Parvibacter, no_norank_f_Coriobacteriaceae*, *Enterorhabdus*, and *Collinsella*; and 2) class: *Betaproteobacteria* → order: *Burkholderiales* → family: *Alcaligenaceae* → genus: *Sutterella*. Further LEfSe results (Fig. 7B) showed that 30 significant enrichment taxa with LDA scores > 2 in response to CAL treatment were found, which indicated that CAL treatment had the greatest impact on the richness of bacteria. The top 3 significantly enriched taxa of *g_Lachnoclostridium, g_Parabacteroides* and *c_Actinobateria* belonged to the *Proteobacteria* or *Actinobacteria* phylum. LEFse analysis further confirmed that *Actinobacteria* was a phylum that was closely related to the effectiveness of SWCA treatment.

To determine whether the metabolic status of different animal groups had any effects on the gut microbial community structure,

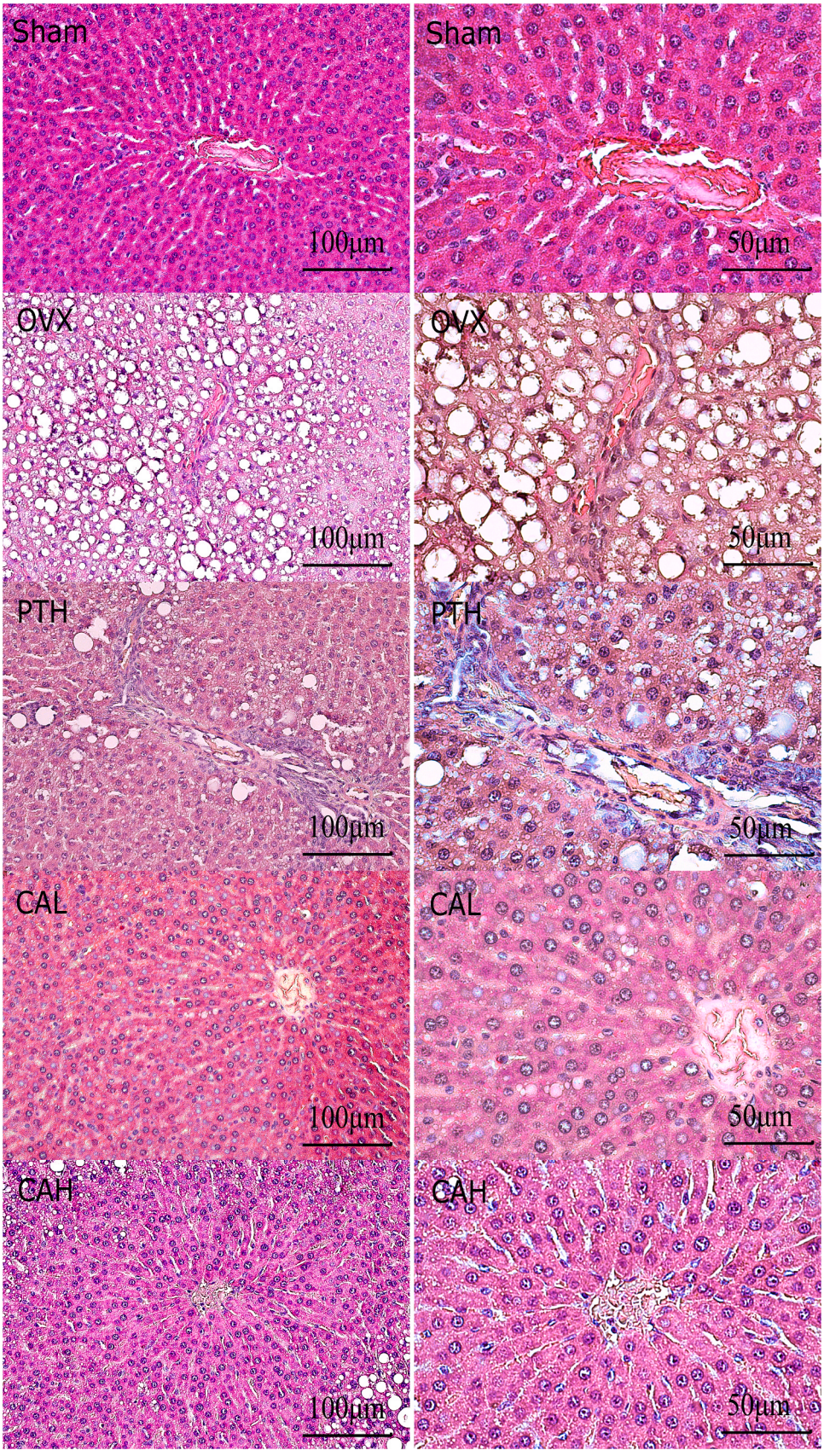

Fig. 2. Histopathological analysis of the liver sections of rats upon different treatments at 100 × (100 μm) and 200 × (50 μm). Four-month-old SD rats were subjected to the following treatment for 10 weeks after ovariectomy: Sham, Sham-operated, vehicle-treated, $n = 10$; OVX, ovariectomized, vehicle-treated, $n = 10$; PTH, ovariectomized, 1.8 μg/kg, $n = 8$; CAL, ovariectomized, low-dose SWCA fraction (140 mg/kg), $n = 10$; CAH, ovariectomized, high-dose SWCA fraction (280 mg/kg), $n = 10$.

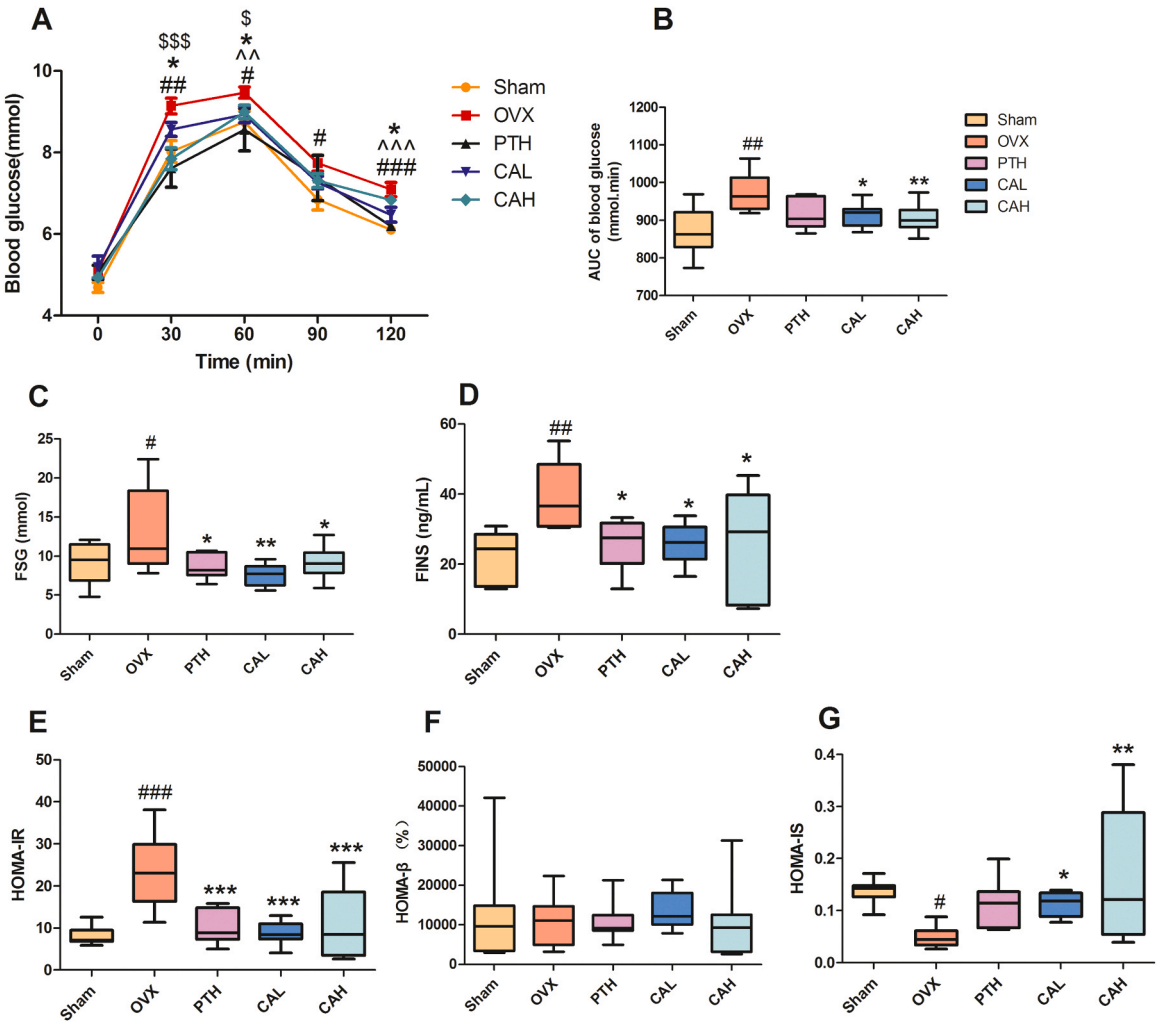

Fig. 3. Effects of SWCA on HOMA and insulin actions. (A) the levels of blood glucose at different time points; (B) AUC of blood glucose; (C) FSG; (D) FINS; (E)HOMA-IR; (F) HOMA-β; (G) HOMA-IS. Four-month-old SD rats were subjected to the following treatment for 10 weeks after ovariectomy: Sham, Sham-operated, vehicle-treated, $n = 10$; OVX, ovariectomized, vehicle-treated, $n = 10$; PTH, ovariectomized, 1.8 μg/kg, $n = 8$; CAL, ovariectomized, low-dose SWCA fraction (140 mg/kg), $n = 10$; CAH, ovariectomized, high-dose SWCA fraction (280 mg/kg), $n = 10$. Results were expressed as mean ± SEM. For A, in OVX group, # $P < 0.05$, ## $P < 0.01$, ### $P < 0.001$ versus Sham at the same time point; in PTH treatment group, ^^ $P < 0.01$, ^^^ $P < 0.001$ versus OVX at the same time point; in CAL treatment group, *$P < 0.05$ versus OVX at the same time point; in CAH treatment group, $ $P < 0.05$, $$$ $P < 0.001$ versus OVX at the same time point. For B-G, # $P < 0.05$, ## $P < 0.01$, ### $P < 0.001$ versus Sham, *$P < 0.05$, ** $P < 0.01$, *** $P < 0.001$ versus OVX by One-Way ANOVA followed with the Tukey's post-hoc test.

correlation analysis of serum biochemistries and bacterial genera was performed. The relationships of the serum TC, TG, LCL-C, HDL-C, ALT, AST, TBIL, ALB, HOMA-IR, TNF-α, IL-1β, IL-1α, IL-6, IL-22 and MCP-1, and the top 50 genera in relative richness were shown in Fig. 8. The biochemistries of lipid metabolic disorder, liver functions and insulin resistance, and proinflammatory cytokines showed relationships with the microbial community structure, especially IL-22 and TNF-α, which had a greater impact on the microbial structure (Fig. 8A). HDL-C was inversely correlated with the other serum biochemistries, which is consistent with their different physiological functions. The heatmap in Fig. 8B showed that the significantly decreased abundances of *Ruminococcaceae_UCG-014* and *[Eubacterium]_coprostanoligenes_group* in response to CAL treatment (Fig. 6B) were positively correlated with TNF-α, TC, TG, IL-22, HOMA-IR, AST and ALT. Conversely, the microbes of *Adlercreutzia*, *Anaerotruncus*, *Barnesiella*, *Enterococcus*, *Lanchnoclostridium*, *Lachnospiraceae_nk4B4_group* and *Lachnospiraceae_UCG-01* which were negatively correlated with serum TNF-α, LDL-C, ALB and AST, were significantly enriched in the CAL treatment group (Fig. 6B).

4. Discussion

Although some components identified in *Sambucus williamsii* Hance, such as α- and β-amyrin [18], betulinic acid [40] and linoleic acid [20], have been reported to have anti-inflammatory, anti-diabetic, anti-glycemic or hypolipidemic activities, the actions of the lignan-rich fraction from *S. williamsii* on lipid metabolism and insulin resistance and the underlying mechanism are still unclear. In this study, we systematically investigated the anti-dyslipidemia and anti-insulin resistance effects of SWCA from *S. williamsii* in ovariectomized rats, and these effects were correlated with gut microbial structure. Our results showed that the metabolic disorders and inflammation in response to estrogen depletion were closely related to gut microbiota. SWCA alleviated dyslipidemia, improved liver functions, prevented glucose tolerance and insulin actions, attenuated system inflammation and improved the intestinal barrier in OVX rats. It also induced a high abundance of *Actinobacteria*, and restored the microbiota composition.

Our results were in consistent with previous findings [41,42] and confirmed that ovariectomy induced body weight gain, and increased serum and hepatic TC, TG, LDL-C and insulin resistance [43,44]. Parathyroid hormone (PTH) was positively correlated with lipolysis of

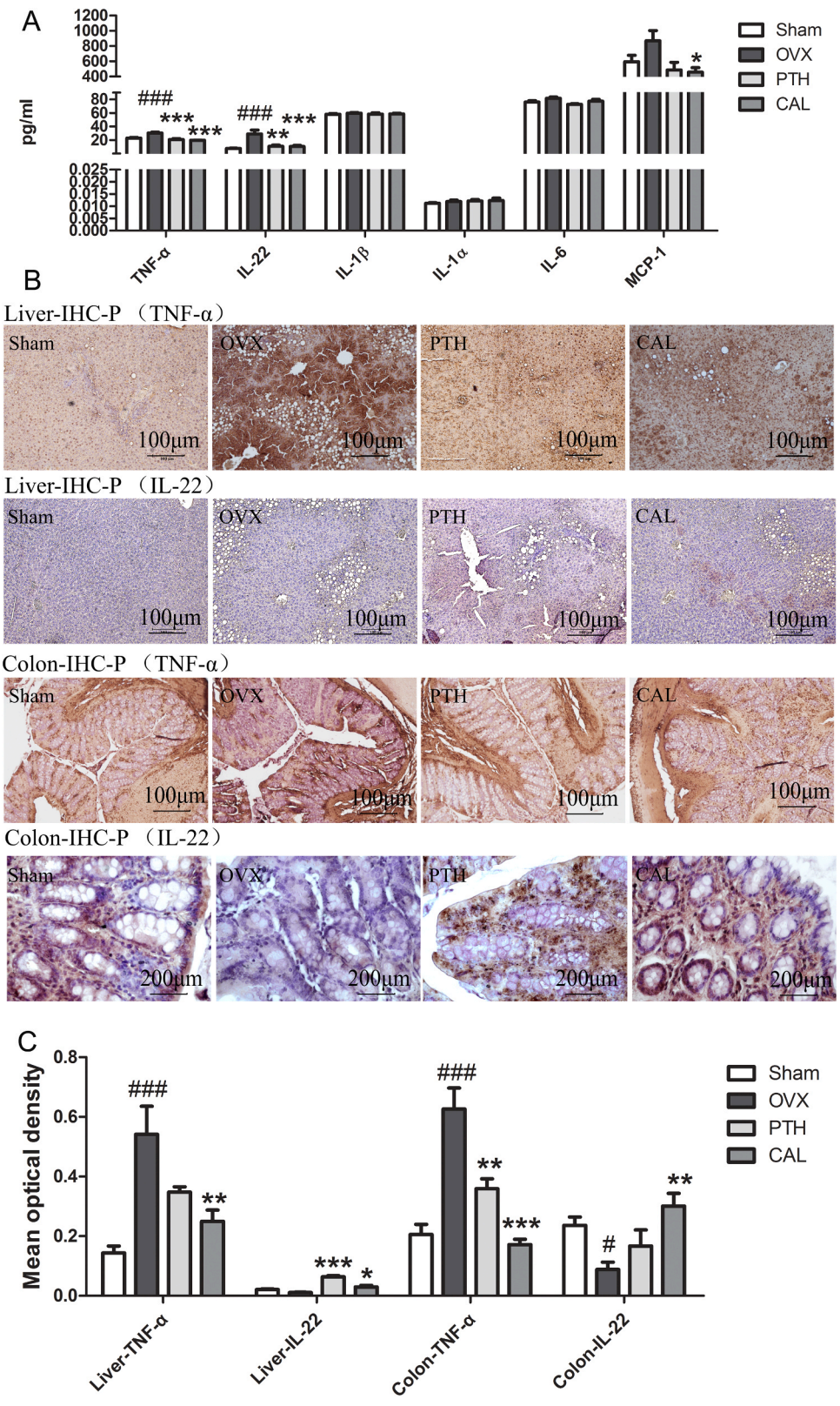

Fig. 4. The effects of SWCA on inflammation in serum, liver and colon. (A) the level of TNF-α, IL-22, IL-1β, IL-1α, MCP-1 and IL-6 in serum; (B) immunohistological staining of TNF-α and IL-22 in liver and colon sections at 100 × and 200 × magnification; (C) mean optical density of TNF-α and IL-22 expressions in liver and colon. Four-month-old SD rats were subjected to the following treatment for 10 weeks after ovariectomy: Sham, Sham-operated, vehicle-treated, $n = 10$; OVX, ovariectomized, vehicle-treated, $n = 10$; PTH, ovariectomized, 1.8 μg/kg, $n = 8$; CAL, ovariectomized, low-dose SWCA fraction (140 mg/kg), $n = 10$; CAH, ovariectomized, high-dose SWCA fraction (280 mg/kg), $n = 10$. Results were expressed as mean ± SEM. ### $P < 0.001$ versus Sham, *$P < 0.05$, ** $P < 0.01$, *** $P < 0.001$ versus OVX by One-Way ANOVA followed with the Tukey's post-hoc test.

adipose tissue and influenced glucose metabolism in postmenopausal women [32,45,46]. Although PTH significantly altered some parameters of lipid and glucose metabolism, its effects were not as potent as those induced by the lignan-rich fraction SWCA. SWCA significantly reversed the deteriorations of lipid and glucose metabolism in ovariectomy rats, but it did not alter their body weight. Similarly, Fayaz et al., reported that cinnamon extract combined with high endurance training alleviated insulin resistance and metabolic dysfunctions and lowered visceral fat, but did not influence the body weight of OVX rats [16]. Although obesity is strongly associated with dyslipidemia and insulin resistance, lean subjects also encounter these disorders, a phenomenon that was initially observed in an Asian population [47]. A meta-analysis by

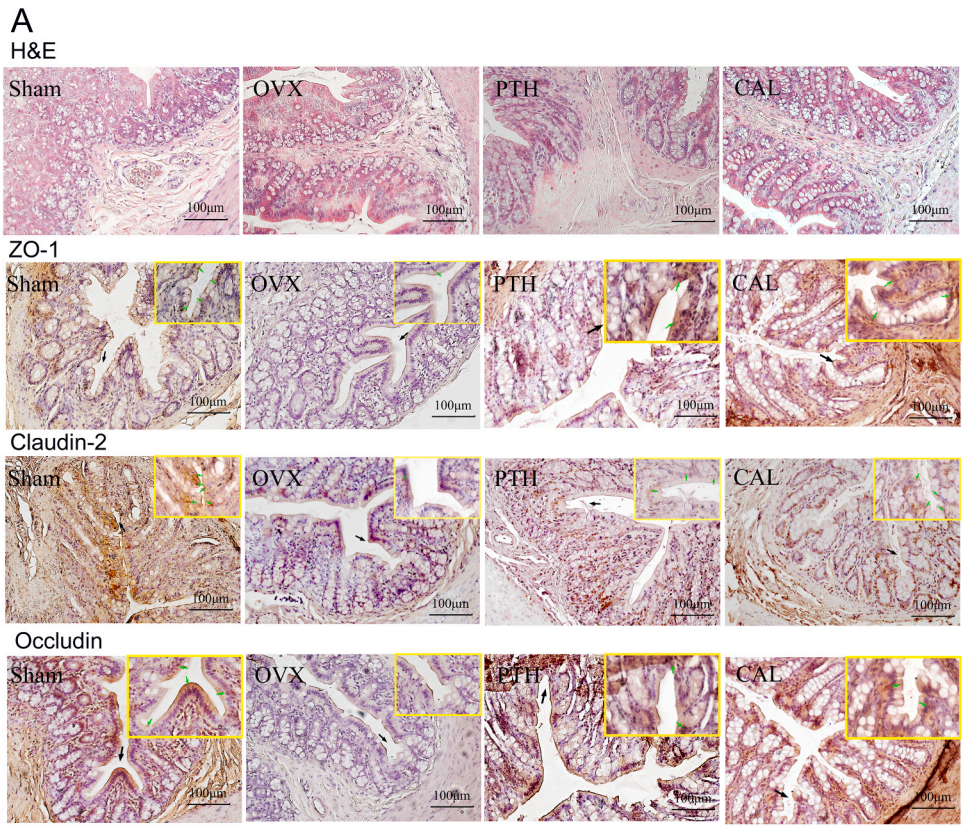

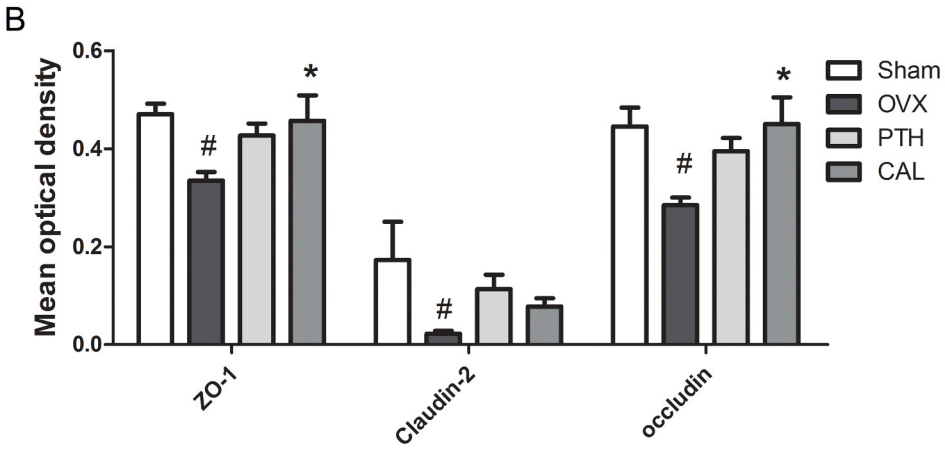

Fig. 5. The effects of SWCA on intestinal barriers. (A) the H&E staining of colon and immunohistological staining of ZO-1, Caludin-2 and Occludin at 200 × and 600 × magnification; (B) mean optical density of ZO-1, Caludin-2 and Occludin. Four-month-old SD rats were subjected to the following treatment for 10 weeks after ovariectomy: Sham, Sham-operated, vehicle-treated, $n = 10$; OVX, ovariectomized, vehicle-treated, $n = 10$; PTH, ovariectomized, 1.8 μg/kg, $n = 8$; CAL, ovariectomized, low-dose SWCA fraction (140 mg/kg), $n = 10$; CAH, ovariectomized, high-dose SWCA fraction (280 mg/kg), $n = 10$. Results were expressed as mean ± SEM. # $P < 0.05$ versus Sham, *$P < 0.05$, versus OVX by One-Way ANOVA followed with the Tukey's post-hoc test.

Sookoian and Pirola on the risk factors associated with lean and obese patients with non-alcoholic fatty liver disease (NAFLD) concluded that lean patients, had significant increase in plasma glucose and HOMA-IR, blood lipids and total cholesterol, and possessed excess of abdominal adipose tissue even though their body weight was normal [48]. All the above findings indicated that body fat, not body weight, was a critical factor modulating lipid metabolism and insulin actions. The current study demonstrated the protective effects of SWCA against ovariectomy-induced lipid and glucose disorder. Its effects on body fat depots will be explored in our future study.

System inflammation was observed in post-menopausal women due to the deficiency of oestrogen [49]. Consistently, in this study, TNF-α was significantly increased in the serum, liver and colon of OVX rats, while SWCA treatment significantly attenuated these high levels of TNF-α in OVX rats. Interestingly, the level of IL-22 significantly was increased in serum of OVX rats, but its expressions were obviously decreased in the liver and colon of OVX rats. SWCA significantly reversed these changes in IL-22 induced by OVX in serum, liver and colon. IL-22 is a proinflammatory cytokine produced by innate lymphocyte cells in mucosa, especially in the intestine, and its receptor is restricted to specific tissues, such as hepatocytes and epithelial cells of the intestinal tract. IL-22 could play either a protective or pathogenic role, depending on the specific tissue and disease state. IL-22 expression protects hepatocytes in a variety of chemical-induced liver damage models [50]. It protects against hepatocellular injury, necrosis and apoptosis in T-cell-dependent hepatitis, ameliorates alcoholic fatty liver damage in alcohol-induced liver injury, and promotes liver progenitor cell proliferation in chronic hepatics B virus infection, while it promotes liver tumor cell growth both *in vitro* and *in vivo* [51,52]. IL-22 also promotes epithelial proliferation to restore epithelial barrier function, leading to limited bacterial replication and dissemination in many infection models [53,54]. In this study, we found that IL-22 plays different roles in the whole blood system and specific tissues. The actions of SWCA in the modulating of the pro-inflammatory cytokines of

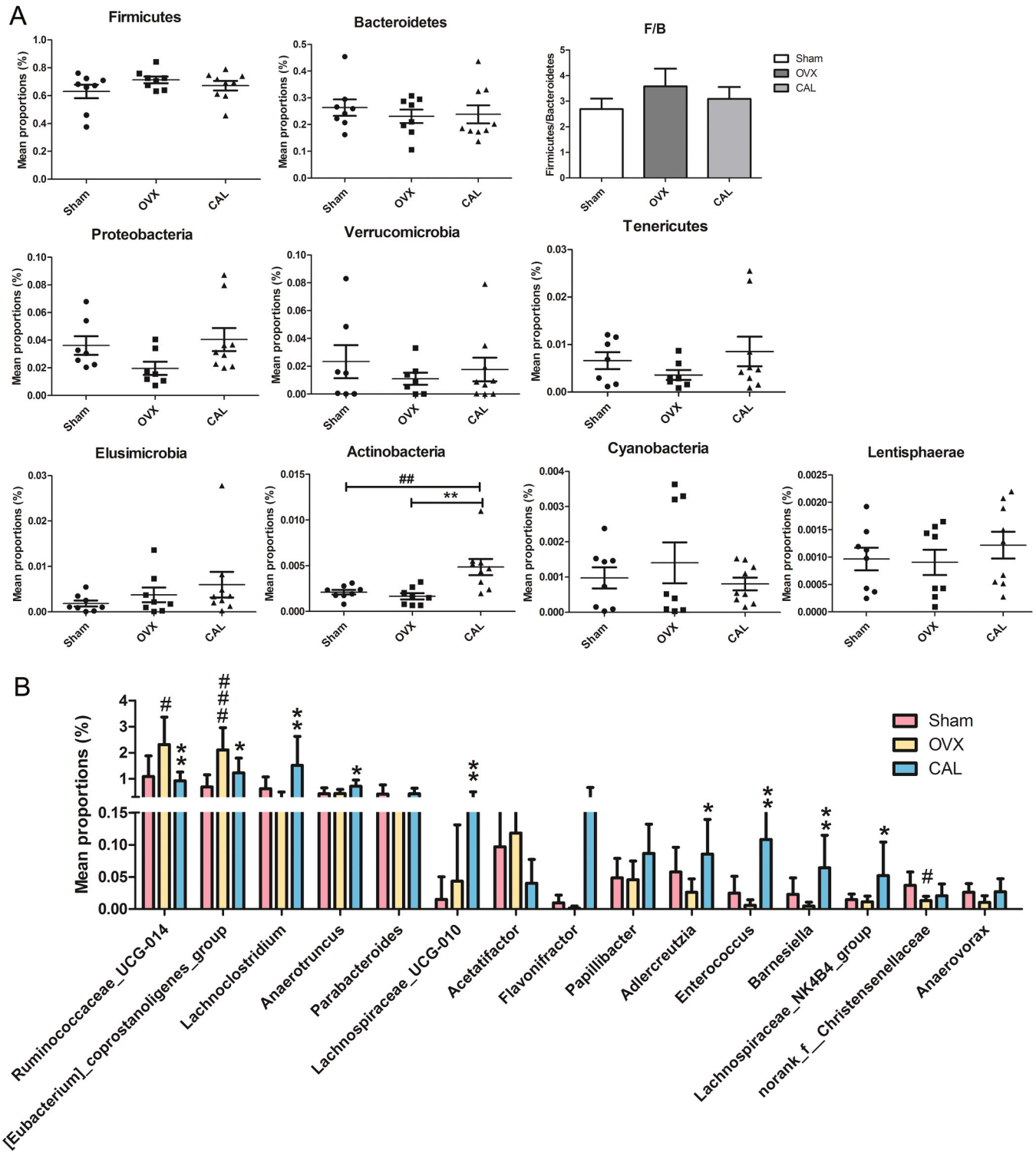

Fig. 6. The effects of SWCA on bacterial compositions in different groups at phylum and genus levels. (A) the relative abundance of gut microbiota at phylum levels; (B) the relative abundance of the top 15 significantly changed gut microbiota at genus levels. Sham, Sham-operated, vehicle-treated; OVX, ovariectomized, vehicle-treated; CAL, ovariectomized, low-dose SWCA fraction (140 mg/kg). $n = 10$ for each group. Results were expressed as mean ± SD. # $P < 0.05$, ## $P < 0.01$, ### $P < 0.001$ versus Sham, *$P < 0.05$, ** $P < 0.01$ versus OVX by Kruskal-Wallis H test.

IL-22 and TNF-α might partially explain its beneficial effects on metabolic disorders.

The intestinal barrier is critical for health by preventing the penetration of macromolecules and potentially pathogenic microorganisms. Some studies identified increased colonic permeability in both *in vivo* and *ex vivo* rodent models of estrogen deficiency [55] and intestinal barrier dysfunction is correlated to various inflammatory diseases, such as Crohn's disease and ulcerative colitis [56]. It's a possible reason for the increased inflammatory cytokines in menopause that some antigens enter to submucosa due to the intestinal barrier disturbance induced by estrogen withdraw. Intestinal tight junction proteins such as occludin, claudins and zonula occludins (ZO) are crucial for maintaining the

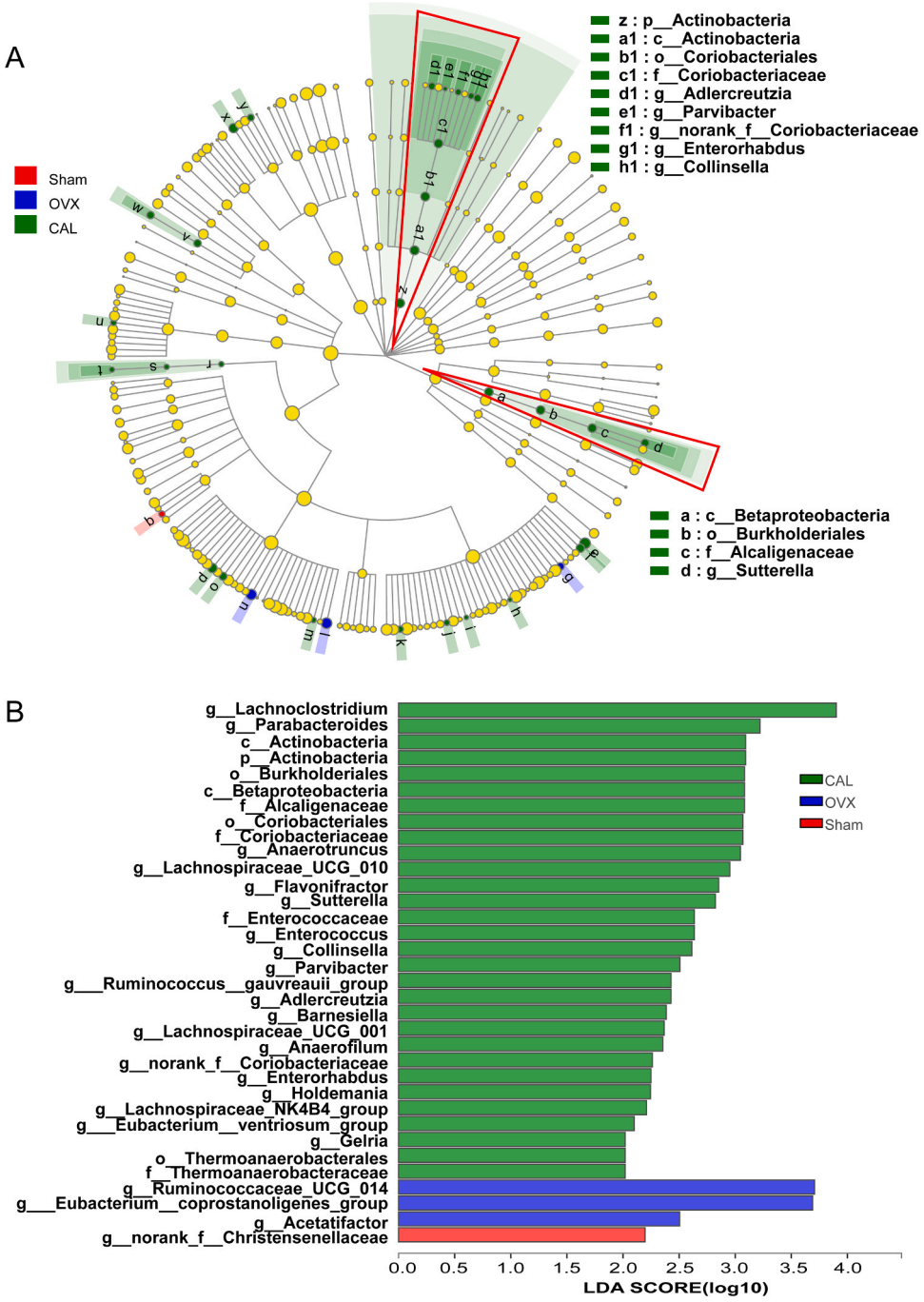

Fig. 7. LEfSe (Linear discriminant analysis effects size) analysis of gut microbiota in each group. (A) cladogram of LefSe analysis; (B) LDA scores in each group. Sham, Sham-operated, vehicle-treated; OVX, ovariectomized, vehicle-treated; CAL, ovariectomized, low-dose SWCA fraction (140 mg/kg). $n = 10$ for each group.

barrier integrity and protective function against intestinal antigens. In the present study, oestrogen depletion decreased the expressions of intestinal tight junction proteins ZO-1, Claudin-2 and Occludin, an observation that was supported by the findings of Chen et al. [57]. SWCA treatment significantly restored the decreases in intestinal junction proteins, thus protecting the gut barrier, which might explain the modulating effects of SWCA on pro-inflammatory cytokines.

There is accumulated evidence showing that gut microbiota plays a key role in the development of metabolic diseases, such as obesity, diabetes, alcoholic liver disease and nonalcoholic fatty liver disease [58]. The composition and structure of gut microbiota is determined by 16s rRNA gene sequencing. The *Firmicutes* to *Bacteroidetes* ratio is generally used to indicate the status of metabolic diseases. Increased ratio of F/B was associated with obesity in humans and mice, diabetes (type I) in mice and dyslipidemia in mice [59], while type 2 diabetes without obesity was related to a decreased ratio of F/B in human and mice [60]. Our results showed that ovariectomy slightly increased the relative abundance ratio of *Firmicutes* to *Bacteroidetes* compared with the Sham group, while SWCA treatment exhibited a mild decreasing trend of F/B in OVX rats, results that were in line with some previous studies. Interestingly, in response to SWCA treatment, the phylum of *Actinobacteria* was significantly increased compared with both the Sham and OVX groups. These bacteria help to digest food in most of the animals. *Actinobacteria* is able to break down different food ingredients such as carbohydrate, protein, lipid and glycan into useable form and maintain a continuous supply of calories to the body [61]. A metabolomics study

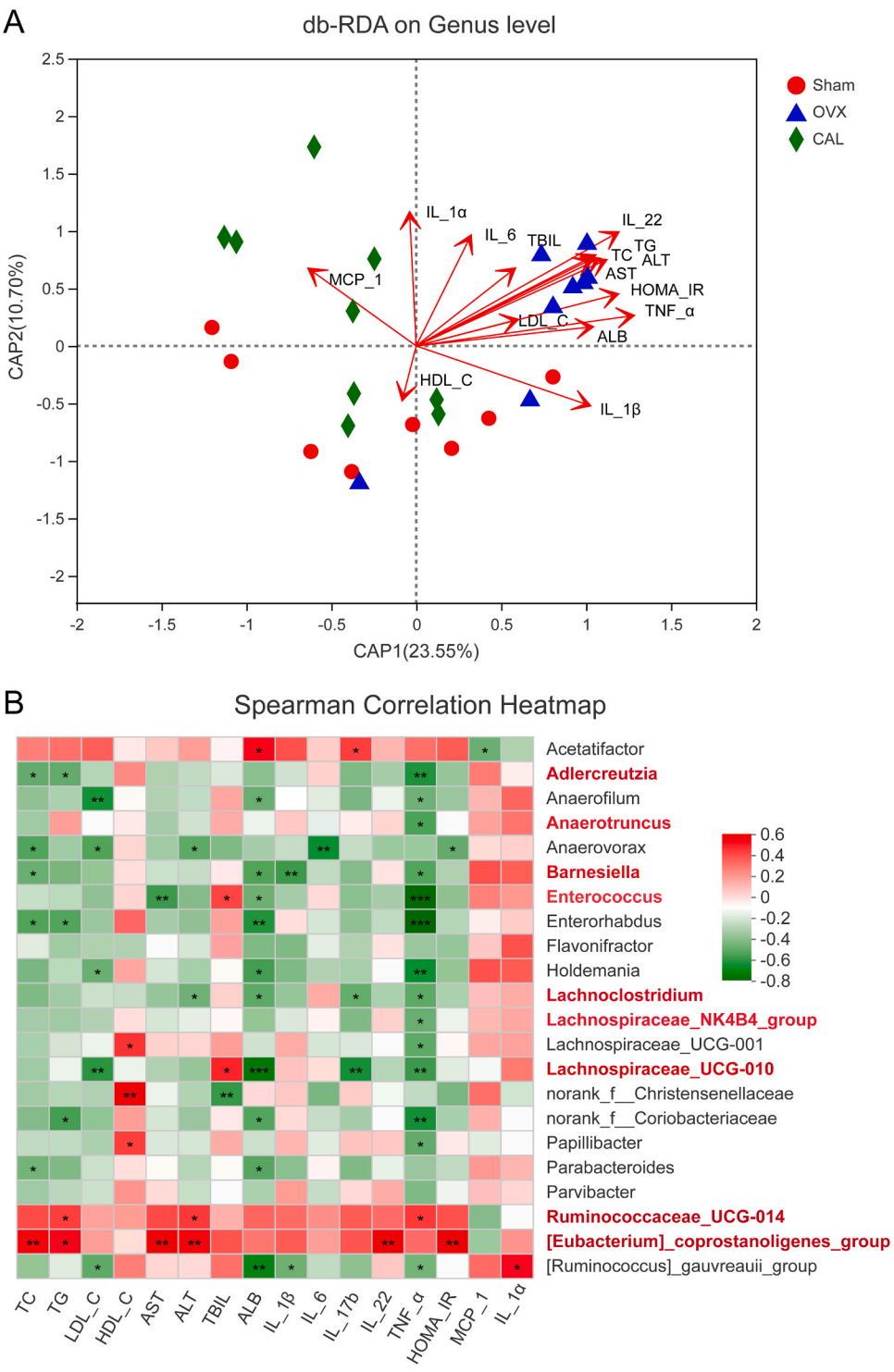

Fig. 8. The correlation between relative abundance of top 50 taxa and serum indicators at genus level. (A) db-RDA analysis. The lengths of the red arrows represent the influence of the serum indicators on gut composition, the angle between the arrows of serum indicators represents the positive (acute angle) and negative correlations (obtuse angle); (B) Spearman correlation heatmap. Red, positive correlation; Green, negative correlation. $^{*}P < 0.05$, $^{**}P < 0.01$, $^{***}P < 0.001$. (For interpretation of the references to colour in this figure legend, the reader is referred to the web version of this article.)

was carried out and the in-house results showed that a high serum enterolactone (an intestinal metabolite of lignans) level was observed in OVX rats upon SWCA treatment for 12 weeks but not in the Sham or OVX vehicle groups. We deduced that high abundance of *Actinobacteria* might promote the transformation of lignans in gut, which may account for the beneficial effects of SWCA on metabolism. Further metagenome of gut microbiota of SWCA in OVX rats will be performed to investigate the metabolic pathways that are related to the gut microbial community.

There is evidence suggesting that the gut microbiome accounts for 6% of the variance in triglycerides and 4% in high-density lipoproteins, independent of age, sex and genetic risk factors [62]. A species of Eubacterium coprostanoligenes ATCC 51222 in *Eubacterium* genus has been found to be cholesterol-reducing barium, and it can reduce cholesterol intake by breaking down cholesterol into coprostanol [63]. Yang et al. reported that the genus of *[Eubacterium]_coprostanoligenes_group* and *Ruminococcaceae_UCG_014* were decreased in rats with high fat diet-induced obesity, but direct correlations of these two genera and lipid metabolic indicators were missing [64]. We found that *[Eubacterium]_coprostanoligenes_group* and *Ruminococcaceae_UCG_014* were significantly increased in ovariectomized rats, while they were

decreased in the SWCA treatment group. In addition, *[Eubacterium]_coprostanoligenes_group* and *Ruminococcaceae_UCG_014* was positively correlated with serum TNF-α, TG and ALT. It should be clarified that *[Eubacterium]_coprostanoligenes_group* is a genus that belongs to *Ruminococaceae* family, while *Eubacterium coprostanoligenes* is a species that belongs to *Eubacterium* genus and *Eubacteriaceae* family. Although Eubacterium coprostanoligenes has the ability to convert cholesterol to coprostanol, *[Eubacterium]_coprostanoligenes_group* may not have the ability to do so. Furthermore, the metabolic dysfunctions induced by high fat diet and those induced by ovariectomy are very different. The Spearman correlation heatmap in the current study showed obvious relationship of *Ruminococcaceae_UCG-014* *[Eubacterium]_coprostanoligenes_group*, *Adlercrutzia*, *Anaerotruncus*, *Barnesiella*, *Lachnospiraceae_nk4B4_group*, *Lachnospiraceae_UCG-010*, *Lanchnoclostridium* and *Enterococcus* with metabolic indictors in ovariectomy rats. Further culture and purification of bacterial species in *[Eubacterium]_coprostanoligenes_group* in vitro is needed to identify their actions on metabolism.

Consumption of lignan-rich vegetables, fruit and whole-grain products is helpful for protecting human from chronic diseases [65,66]. Several studies have addressed the beneficial effects of lignan-rich diet on lipid improvement and glycemic control in humans or in animals [67,68]. Post-menopausal women (average age 56.8) with high dietary lignan intake could lower body mass index (BMI) and total body fat mass, improve glucose disposal rate and have a high level of plasma enterolactone compared with women in the low lignan intake group [67]. In the current study, consistent with some previous lignan-related reports, we found that the lignan-rich fraction SWCA from *S. williamsii* alleviated dyslipidemia, improved liver functions, and prevented glucose tolerance and insulin actions.

5. Conclusion

The present study systematically demonstrated that the lignan-rich fraction, SWCA, from *Sambucus williamsii Hance* significantly alleviated dyslipidemia, improved liver functions, prevented glucose tolerance and insulin actions, attenuated system inflammation, improved intestinal barrier in OVX rats. In addition, changes in the composition of gut microbiota were attributed to the effects of SWCA on metabolic disorders. We are the first to report the protective effects of the lignan-rich fraction form *S. williamsii* on dyslipidemia and insulin resistance. Our findings provide strong evidence for the application of this lignan-rich fraction to patients with menopausal lipid disorder or insulin resistance-related diseases.

Conflict of interest statement

The authors declare that there are no conflicts of interest

Acknowledgement

The study was supported by Shenzhen Basic Research Program (JCYJ20170818104152702), National Natural Science Foundation of China (81903616), The Hong Kong Midstream Research Programme for Universities (MRP/012/18X), General Research Fund (Project No. 15302718) and Collaborative Research Fund (CRF Grant No. C5031-14E, C5033-19E) of the Research Grant Council of the Hong Kong Special Administrative Region, the Hong Kong Chinese Materia Medica Standards Project, Hong Kong Polytechnic University financial support (Project No. YBU0), the Large Equipment Funds and University Research Facility in Chemical and Environmental Analysis and Life Sciences of the Hong Kong Polytechnic University.

Appendix A. Supporting information

Supplementary data associated with this article can be found in the online version at doi:10.1016/j.biopha.2021.111372.

References

[1] R.B. Pothineni, G.S. Guntuku, P.M. Ranjit, New atherogenic indices: assessment of cardio vascular risk in post menopausal dyslipidemia, Asian J. Med. Sci. 6 (2015) 25–32.
[2] J.A. Cauley, K. Ruppert, Y. Lian, J.S. Finkelstein, C.A. Karvonen-Gutierrez, S. D. Harlow, J.C. Lo, S.M. Burnett-Bowie, A. Karlamangla, G.A. Greendale, Serum sex hormones and the risk of fracture across the menopausal transition: study of women's health across the nation, J. Clin. Endocrinol. Metab. 104 (2019) 2412–2418.
[3] J. Almeida, Menopause and the metabolic syndrome, Panacea J. Med. Sci. 5 (2015) 158–160.
[4] H.J. Teede, C. Lombard, A.A. Deeks, Obesity, metabolic complications and the menopause: an opportunity for prevention, Climacteric 13 (2010) 203–209.
[5] A. Veloso, E. Gama, L. Maifrino, Treatments used in menopausal women susceptible to dyslipidemia and diabetes, J. Morphol. Sci. 34 (2018) 207–213.
[6] S. Faria Tda, A.L. Correia Jr., T.L. dos Anjos, M.B. Aguila, C.A. Mandarim-de-Lacerda, Adverse association between obesity and menopause in mice treated with bezafibrate, a pan peroxisome proliferator-activated receptor agonist, Menopause 20 (2013) 1264–1274.
[7] K. Veras, F.N. Almeida, R.T. Nachbar, D.S. de Jesus, J.P. Camporez, A.R. Carpinelli, J.H. Goedecke, C.R. de Oliveira Carvalho, DHEA supplementation in ovariectomized rats reduces impaired glucose-stimulated insulin secretion induced by a high-fat diet, FEBS Open Bio 4 (2014) 141–146.
[8] M. Nagamani, A. Szymajda, V. Sepilian, R. Urban, C. Gilkison, Effects of raloxifene on insulin sensitivity, β-cell function, and hepatic insulin extraction in normal postmenopausal women, Fertil. Steril. 89 (2008) 614–619.
[9] N. Alexopoulos, B.H. Melek, C.D. Arepalli, G.R. Hartlage, Z. Chen, S. Kim, A. E. Stillman, P. Raggi, Effect of intensive versus moderate lipid-lowering therapy on epicardial adipose tissue in hyperlipidemic post-menopausal women: a substudy of the BELLES trial (Beyond Endorsed Lipid Lowering with EBT Scanning), J. Am. Coll. Cardiol. 61 (2013) 1956–1961.
[10] L. Kang, C.H. Chen, M.H. Wu, J.K. Chang, F.M. Chang, J.T. Cheng, 17beta-estradiol protects against glucosamine-induced pancreatic beta-cell dysfunction, Menopause 21 (2014) 1239–1248.
[11] I. Khorsand, R. Kashef, M. Ghazanfarpour, E. Mansouri, S. Dashti, T. Khadivzadeh, The beneficial and adverse effects of raloxifene in menopausal women: a mini review, J. Menopausa Med. 24 (2018) 183–187.
[12] V. Scheid, V. Tuffrey, M. Bovey, Chinese herbal medicine for treating menopausal symptoms in London women: developing a good practice protocol via the factor analysis of prescribing patterns in a clinical study, Complement. Ther. Med. 32 (2017) 33–40.
[13] M. Guo, Y. Liu, Z.-Y. Gao, D.-Z. Shi, Chinese herbal medicine on dyslipidemia: progress and perspective, Evid. Based Complement. Altern. Med. 2014 (2014) 1–11.
[14] C. Liu, Y. Huang, Chinese herbal medicine on cardiovascular diseases and the mechanisms of action, Front. Pharmacol. 7 (2016).
[15] X. Hu, M. Wang, W. Bei, Z. Han, J. Guo, The Chinese herbal medicine FTZ attenuates insulin resistance via IRS1 and PI3K in vitro and in rats with metabolic syndrome, J. Transl. Med. 12 (2014) 47.
[16] E. Fayaz, A. Damirchi, N. Zebardast, P. Babaei, Cinnamon extract combined with high-intensity endurance training alleviates metabolic syndrome via non-canonical WNT signaling, Nutrition 65 (2019) 173–178.
[17] H.H. Xiao, Y. Zhang, R. Cooper, X.S. Yao, M.S. Wong, Phytochemicals and potential health effects of Sambucus williamsii Hance (Jiegumu), Chin. Med. 11 (2016) 36.
[18] R.C.R. Lima-Júnior, D.I.M. Sousa, G.A. Brito, G.M. Cunha, M.H. Chaves, V.S. N. Rao, F.A. Santos, Modulation of acute visceral nociception and bladder inflammation by plant triterpene, α,β-amyrin in a mouse model of cystitis: role of tachykinin NK1-receptors, and K^+ ATP channels, Inflamm. Res. 56 (2007) 1–8.
[19] Y. Zhang, Q. Li, H.Y. Wan, H.H. Xiao, W.P. Lai, X.S. Yao, M.S. Wong, Study of the mechanisms by which *Sambucus williamsii* HANCE extract exert protective effects aginst ovariectomy-induced osteoporosis in vivo, Osteoporos. Int. 22 (2011) 703–709.
[20] H. Lv, S.S. Chen, X.L. Xu, M.M. Zhu, W.F. Zhao, K.W. Liu, K.H. Liu, Isolation of linoleic acid from sambucus williamsii seed oil extracted by high pressure fluid and its antioxidant, antiglycemic, hypolipidemic activities, Int. J. Food Eng. 11 (2015) 383–391.
[21] H. Kuang, Z. Tang, X. Wang, B. Yang, Z. Wang, Q. Wang, Chemical constituents from Sambucus williamsii Hance fruits and hepatoprotective effects in mouse hepatocytes, Nat. Prod. Res. 32 (2018) 2008–2016.
[22] H.H. Xiao, T.T. Sham, C.O. Chan, M.H. Li, X. Chen, Q.C. Wu, D.K.W. Mok, X.S. Yao, M.S. Wong, A metabolomics study on the bone protective effects of a lignan-rich fraction from Sambucus Williamsii Ramulus in aged rats, Front. Pharmacol. 9 (2018) 932.
[23] Q. Junjie, L. Ruiqiang, R. Jeroen, A. Manimozhiyan, B. Kristoffer Solvsten, M. Chaysavanh, N. Trine, P. Nicolas, L. Florence, Y. Takuji, R.M. Daniel, L. Junhua, X. Junming, L. Shaochuan, L. Dongfang, C. Jianjun, W. Bo, L. Huiqing, Z. Huisong, X. Yinlong, T. Julien, L. Patricia, B. Marcelo, B. Jean-Michel, H. Torben, P. Denis Le, L. Allan, H.B. Nielsen, P. Eric, R. Pierre, S.-P. Thomas, T. Keith, Z. Hongmei, Y. Chang, L. Shengting, J. Min, Z. Yan, L. Yingrui, Z. Xiuqing, L. Songgang, Q. Nan, Y. Huanming, W. Jian, B. Søren, D. Joel, G. Francisco, K. Karsten, P. Oluf, P. Julian, W. Jean, B. Peer, S.D. Ehrlich, W. Jun, A human gut

microbial gene catalogue established by metagenomic sequencing, Nature 464 (2010) 59–65.
[24] E.L. Ruth, J.T. Peter, K. Samuel, I.G. Jeffrey, Human gut microbes associated with obesity, Nature 444 (2006) 1022–1023.
[25] J.T. Peter, H. Micah, Y. Tanya, L.C. Brandi, D. Alexis, E.L. Ruth, L.S. Mitchell, J. J. William, A.R. Bruce, P.A. Jason, E. Michael, H. Bernard, C.H. Andrew, K. Rob, I. G. Jeffrey, A core gut microbiome in obese and lean twins, Nature 457 (2009) 480–484.
[26] X. Wu, C. Ma, L. Han, M. Nawaz, F. Gao, X. Zhang, P. Yu, Ca Zhao, L. Li, A. Zhou, J. Wang, J. Moore, B. Cherie Millar, J. Xu, Molecular characterisation of the faecal microbiota in patients with type ii diabetes, Curr. Microbiol. 61 (2010) 69–78.
[27] T. Geach, Gut microbiota improves dysglycaemia, Nat. Rev. Endocrinol. 12 (2016) 310.
[28] R.H. Michael, S.G. Wendy, A complex microworld in the gut: gut microbiota and cardiovascular disease connectivity, Nat. Med. 18 (2012) 1188–1189.
[29] C. Zhang, M. Zhang, S. Wang, R. Han, Y. Cao, W. Hua, Y. Mao, X. Zhang, X. Pang, C. Wei, G. Zhao, Y. Chen, L. Zhao, Interactions between gut microbiota, host genetics and diet relevant to development of metabolic syndromes in mice, ISME J. 4 (2010) 232–241.
[30] H.H. Xiao, J. Lv, D. Mok, X.S. Yao, M.S. Wong, R. Cooper, NMR applications for botanical mixtures: the use of HSQC data to determine lignan content in Sambucus williamsii, J. Nat. Prod. 82 (2019) 1733–1740.
[31] H.H. Xiao, Y. Dai, H.Y. Wan, M.S. Wong, X.S. Yao, Bone-protective effects of bioactive fractions and ingredients in *Sambucus williamsii* HANCE, Br. J. Nutr. 106 (2011) 1802–1809.
[32] S. Larsson, H.A. Jones, O. Goransson, E. Degerman, C. Holm, Parathyroid hormone induces adipocyte lipolysis via PKA-mediated phosphorylation of hormone-sensitive lipase, Cell. Signal. 28 (2016) 204–213.
[33] T.K. Sinha, P. Thajchayapong, S.F. Queener, D.O. Allen, N.H. Bell, On the lipolytic action of parathyroid hormone in man, Metabolism 25 (1976) 251–260.
[34] J. Lovegrove, J. Wright, W.C. Adiposity, Insulin and lipid metbolism in post-menopausal women, Int. J. Obes. Relat. Metab. Disord. 26 (2002) 475–486.
[35] C. Nagy, E. Einwallner, Study of glucose metabolism in high-fat diet-fed mice using oral glucose tolerance test (OGTT) and insulin tolerance test (ITT), J. Vis. Exp. (2018) 131.
[36] M.M. Lasram, K. Bouzid, I.B. Douib, A. Annabi, N.E. Elj, S.E. Fazaa, J. Abdelmoula, N. Gharbi, Lipid metabolism disturbances contribute to insulin resistance and decrease insulin sensitivity by malathion exposure in wistar rat, Drug Chem. Toxicol. 38 (2015) 227–234.
[38] K.H. Liland, H. Vinje, L. Snipen, Microclass: an R-package for 16S taxonomy classification, BMC Bioinform. 18 (2017) 172.
[39] X. Qian, Y.X. Liu, X. Ye, W. Zheng, S. Lv, M. Mo, J. Lin, W.Q. Wang, W.H. Wang, X. Zhang, M. Lu, Gut microbiota in children with juvenile idiopathic arthritis: characteristics, biomarker identification, and usefulness in clinical prediction, BMC Genom. 21 (2020) 286.
[40] C.L. De Melo, M.G.R. Queiroz, A.C.V. Arruda Filho, A.M. Rodrigues, D.F. De Sousa, J.G.L. Almeida, O.D.L. Pessoa, E.R. Silveira, D.B. Menezes, T.S. Melo, F.A. Santos, V.S. Rao, Betulinic acid, a natural pentacyclic triterpenoid, prevents abdominal fat accumulation in mice fed a high-fat diet, J. Agric. Food Chem. 57 (2009) 8776–88781.
[41] J.A. Lovegrove, K. Silva, J.W. Wright, C.M. Williams, Adiposity, insulin and lipid metabolism in post-menopausal women, Int. J. Obes. 26 (2002) 475–486.
[42] U. Kirtikar, N. Kajale, V. Patwardhan, V. Khadilkar, A. Khadilkar, Cardiometabolic risk in pre- and post-menopausal women with special reference to insulin resistance: a cross-sectional study, J. -Life Health 11 (2020) 22–26.
[43] S.H. Tawfik, B.F. Mahmoud, M.I. Saad, M. Shehata, M.A. Kamel, M.H. Helmy, Similar and additive effects of ovariectomy and diabetes on insulin resistance and lipid metabolism, Biochem. Res. Int. 2015 (2015) 567945–567948.
[44] M.L. Liu, X. Xu, W.Q. Rang, Y.J. Li, H.P. Song, Influence of ovariectomy and 17β-estradiol treatment on insulin sensitivity, lipid metabolism and post-ischemic cardiac function, Int. J. Cardiol. 97 (2004) 485–493.
[45] A. Taniguchi, K. Kataoka, T. Kono, F. Oseko, H. Okuda, I. Nagata, H. Imura, Parathyroid hormone-induced lipolysis in human, J. Lipid Res. 28 (1987) 490–494.
[46] P. D'Amelio, F. Sassi, I. Buondonno, E. Spertino, C. Tamone, S. Piano, D. Zugna, L. Richiardi, G.C. Isaia, Effect of intermittent PTH treatment on plasma glucose in osteoporosis: a randomized trial, Bone 76 (2015) 177–184.
[47] S. Petta, V. Di Marco, R.M. Pipitone, S. Grimaudo, C. Buscemi, A. Craxì, S. Buscemi, Prevalence and severity of nonalcoholic fatty liver disease by transient elastography: genetic and metabolic risk factors in a general population, Liver Int. 38 (2018) 2060–2068.
[48] S. Sookoian, C.J. Pirola, Systematic review with meta-analysis: risk factors for non-alcoholic fatty liver disease suggest a shared altered metabolic and cardiovascular profile between lean and obese patients, Aliment. Pharmacol. Ther. 46 (2017) 85–95.
[49] J. Zhang, H. Wang, S. Yang, X. Wang, Comparison of lipid profiles and inflammation in pre- and post-menopausal women with cerebral infarction and the role of atorvastatin in such populations, Lipids Health Dis. 17 (2018) 20–26.
[50] L.A. Zenewicz, G.D. Yancopoulos, D.M. Valenzuela, A.J. Murphy, M. Karow, R. A. Flavell, Interleukin-22 but not interleukin-17 provides protection to hepatocytes during acute liver inflammation, Immunity 27 (2007) 647–659.
[51] O. Park, H. Wang, H. Weng, L. Feigenbaum, H. Li, S. Yin, S.H. Ki, S.H. Yoo, S. Dooley, F.S. Wang, H.A. Young, B. Gao, In vivo consequences of liver-specific interleukin-22 expression: implications for human liver disease progression, Hepatology 54 (2011) 252–261.
[52] M.A. Cobleigh, M.D. Robek, Protective and pathological properties of IL-22 in liver disease, Am. J. Pathol. 182 (2013) 21–28.
[53] M. Valeri, M. Raffatellu, Cytokines IL-17 and IL-22 in the host response to infection, Pathog. Dis. 74 (74) (2016) ftw111.
[54] Y. Zhuang, P. Cheng, X.F. Liu, L.S. Peng, B.-s Li, T.-t Wang, N. Chen, W.H. Li, Y. Shi, W. Chen, K.C. Pang, M. Zeng, X.H. Mao, S.M. Yang, H. Guo, G. Guo, T. Liu, Q. F. Zuo, H.J. Yang, L.Y. Yang, F.Y. Mao, Y.P. Lv, Q.M. Zou, A pro-inflammatory role for Th22 cells in helicobacter pylori-associated gastritis, Gut 64 (2015) 1368–1378.
[55] J.Y. Li, B. Chassaing, A.M. Tyagi, C. Vaccaro, T. Luo, J. Adams, T.M. Darby, M. N. Weitzmann, J.G. Mulle, A.T. Gewirtz, R.M. Jones, R. Pacifici, Sex steroid deficiency-associated bone loss is microbiota dependent and prevented by probiotics, J. Clin. Investig. 126 (2016) 2049–2063.
[56] J. Libertucci, U. Dutta, S. Kaur, J. Jury, L. Rossi, M.E. Fontes, M.S. Shajib, W. I. Khan, M.G. Surette, E.F. Verdu, D. Armstrong, Inflammation-related differences in mucosa-associated microbiota and intestinal barrier function in colonic Crohn's disease, Am. J. Physiol. Gastrointest. Liver Physiol. 315 (2018) G420–G431.
[57] X. Chen, Z. Zhang, Y. Hu, J. Cui, X. Zhi, X. Li, H. Jiang, Y. Wang, Z. Gu, Z. Qiu, X. Dong, Y. Li, J. Su, Lactulose suppresses osteoclastogenesis and ameliorates estrogen deficiency-induced bone loss in mice, Aging Dis. 11 (2020) 629.
[58] Y. Kang, X. Zhang, Y. Cai, J. Su, X. Kong, Gut microbiota and metabolic disease: from pathogenesis to new therapeutic strategies, Rev. Med. Microbiol. 27 (2016) 141–152.
[59] M. Liu, L. Ma, Q. Chen, P. Zhang, C. Chen, L. Jia, H. Li, Fucoidan alleviates dyslipidemia and modulates gut microbiota in high-fat diet-induced mice, J. Funct. Foods 48 (2018) 220–227.
[60] M. Serino, Molecular paths linking metabolic diseases, gut microbiota dysbiosis and enterobacteria infections, J. Mol. Biol. 430 (2018) 581–590.
[61] J. Wink, F. Mohammadipanah, J. Hamedi, Biology and Biotechnology of Actinobacteria, Springer International AG, Cham, 2017.
[62] J. Fu, M.J. Bonder, M.C. Cenit, E. Tigchelaar-Feenstra, A. Maatman, J.A.M. Dekens, E. Brandsma, J. Marczynska, F. Imhann, R.K. Weersma, L. Franke, T.W. Poon, R. J. Xavier, D. Gevers, M.H. Hofker, C. Wijmenga, A. Zhernakova, The gut microbiome contributes to a substantial proportion of the variation in blood lipids, Circ. Res. 117 (2015) 817–824.
[63] T.A. Freier, D.C. Beitz, L. Li, P.A. Hartman, Characterization of Eubacterium coprostanoligenes sp. nov., a cholesterol-reducing anaerobe, Int. J. Syst. Bacteriol. 44 (1994) 137–142.
[64] X. Yang, W. Mo, C. Zheng, W. Li, J. Tang, X. Wu, Alleviating effects of noni fruit polysaccharide on hepatic oxidative stress and inflammation in rats under a high-fat diet and its possible mechanisms, Food Funct. 11 (2020) 2953–2968.
[65] A. Pan, J. Sun, Y. Chen, X. Ye, H. Li, Z. Yu, Y. Wang, W. Gu, X. Zhang, X. Chen, W. Demark-Wahnefried, Y. Liu, X. Lin, Effects of a flaxseed-derived lignan supplement in type 2 diabetic patients: a randomized, double-blind, cross-over trial, PLoS One 2 (2007), e1148.
[66] C. Rodríguez-García, C. Sánchez-Quesada, E. Toledo, M. Delgado-Rodríguez, J. J. Gaforio, Naturally lignan-rich foods: a dietary tool for health promotion? Molecules 24 (2019) 917.
[67] A.-S. Morisset, S. Lemieux, A. Veilleux, J. Bergeron, S. John Weisnagel, A. Tchernof, Impact of a lignan-rich diet on adiposity and insulin sensitivity in post-menopausal women, Br. J. Nutr. 102 (2009) 195–200.
[68] S.M.D. Dodin, S.C.P.D. Cunnane, B.P.D. Mâsse, A.M.D. Lemay, H.P.D. Jacques, G. M.S. Asselin, J.M.S. Tremblay-Mercier, I.M.D. Marc, B.P.D. Lamarche, F.M. D. Légaré, J.-C.M.D. Forest, Flaxseed on cardiovascular disease markers in healthy menopausal women: a randomized, double-blind, placebo-controlled trial, Nutrition 24 (2008) 23–30.